Elastic buckling of axisymmetric cylindrical shells under axial load using first order shear deformation theory

ARTICLE *in* ZAMM JOURNAL OF APPLIED MATHEMATICS AND MECHANICS: ZEITSCHRIFT FÜR ANGEWANDTE MATHEMATIK UND MECHANIK · NOVEMBER 2012

Impact Factor: 1.16 · DOI: 10.1002/zamm.201200004

Farid mahboubi nasrekani

Shahrood University of Technology

Journal of Applied Mathematics and Mechanics

ZAMM

Zeitschrift für Angewandte Mathematik und Mechanik
Founded by Richard von Mises in 1921

Edited in cooperation with Martin-Luther-Universität Halle-Wittenberg and Gesellschaft für Angewandte Mathematik und Mechanik e. V. (GAMM)

www.zamm-journal.org

WILEY

REPRINT

ZAMM · Z. Angew. Math. Mech. **92**, No. 11 – 12, 937 – 944 (2012) / **DOI** 10.1002/zamm.201200004

Elastic buckling of axisymmetric cylindrical shells under axial load using first order shear deformation theory

F. Mahboubi Nasrekani* **and H. R. Eipakchi****

Mechanical Engineering Faculty, Shahrood University of Technology, Shahrood, I.R. Iran

Received 8 January 2012, revised 3 May 2012, accepted 29 May 2012
Published online 13 July 2012

Key words Buckling analysis, finite elements, analytical solution, perturbation method.

In this paper, the elastic buckling stress of axisymmetric cylindrical shells under uniform axial load is determined analytically by using the first order shear deformation theory. The equilibrium equations are derived by the virtual work principle and then the stability equations are extracted from them. They are systems of differential equations, which are solved analytically by using the perturbation method. The effects of the geometrical properties on the buckling stress are investigated by a parametric study. The results are compared with the finite elements methods.

1 Introduction

The buckling analysis is very important in engineering design especially in thin walled structures. Lorenz (1911) determined the buckling load of a thin cylinder under axial load by using the classical shell theory. Southwell (1913) and von Mises (1914) studied the cylindrical shell buckling under external pressure. Flugge (1932) investigated the buckling of a cylinder under bending load. The Donnell formula (1934) in torsional buckling, the nonlinear theory of von Kármán (1941), the improved theory of Sanders (1963), the shear deformation theory of Reddy (1985) presented too [1]. Cai et al. [2] investigated the effect of imperfection on the buckling strength under axial concentrated loading by using the finite element (FE) method. Khamlichi et al. [3] studied the effect of axisymetric imperfections on the critical load under axial loading analytically. Aghajari et al. [4] calculated the buckling load of a cylinder with varying thickness under external pressure using numerical method and they compared the results with the experimental tests. Abdelmoula et al. [5] determined the non-axisymmetric external buckling pressure for large Batdorf parameter. They used the classical shell theory for analysis. Shen et al. [6] studied the bucking of the composite cylinders with imperfection under axial and torsion loads. They used the classical shell theory and von Kármán kinematic relations. The solution method was the perturbation technique and the numerical method. Shen et al. [7] calculated the buckling load of a FGM cylinder in thermal environments by applying a higher order shear deformation theory and von Kármán kinematic relations. They solved the equations with the asymptotic and numerical methods for large Batdorf parameter. Li et al. [8] investigated the buckling of anisotropic laminated shell under non-uniform external pressure. The solution procedure is similar to [8].

In this paper, the governing equations are extracted based on the first order shear deformation theory by considering the von Kármán kinematic relations. The equilibrium equations are converted to a dimensionless form and the perturbation technique is used to solve these nonlinear equations. Also, an analytical solution for the stability equations are presented. The results are compared with the FE method.

2 Equilibrium equations

A cylindrical shell with the length l, mean radius R, thickness h, is under a uniform axial stress P. The problem is assumed elastic and axisymmetric. According to the first order shear deformation theory, the displacement field is assumed as Eq. (1).

$$U_x(x,z) = u_0(x) + z u_1(x)\,, \quad U_z(xz) = w_0(x). \tag{1}$$

Where x = axial coordinate, z = radial coordinate which it is measured from the middle surface, $U_x(x,z)$ = axial displacement, $U_z(x,z)$ = radial displacement, $u_0(x)$, $u_1(x)$, $w_0(x)$ = unknown functions of x. Figure 1 shows a schematic of the shell.

* Corresponding author E-mail: farid.mn83@gmail.com
** E-mail: hamidre2000@gmail.com

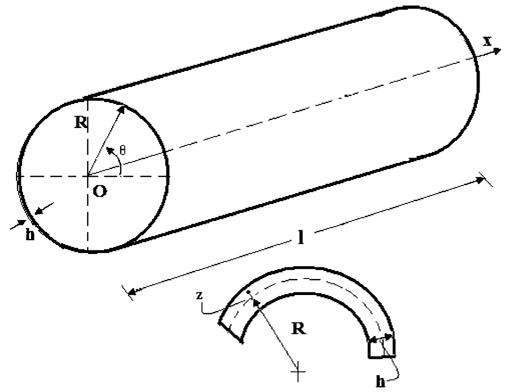

Fig. 1 Schematic of a shell.

According to the von Kármán relations, the kinematic equations for large displacements are [9]:

$$\varepsilon_x = \frac{du_0}{dx} + z\frac{du_1}{dx} + \frac{1}{2}\left(\frac{dw_0}{dx}\right)^2, \quad \varepsilon_\theta = \frac{w_0}{r},$$
$$\gamma_{xz} = \frac{dw_0}{dx} + u_1, \quad \varepsilon_z = \gamma_{x\theta} = \gamma_{\theta z} = 0. \tag{2}$$

The virtual work principle states that $\delta U = \delta W$, where $U =$ strain energy and $W =$ external work. For the elastic case, the strain energy, external work and their variations are:

$$U = \iiint U^* dV, \quad dV = r dr d\theta dx, \quad r = R + z,$$
$$U^* = \frac{1}{2}\left(\sigma_x\varepsilon_x + \sigma_\theta\varepsilon_\theta + \sigma_z\varepsilon_z + \tau_{xz}\gamma_{xz} + \tau_{x\theta}\gamma_{x\theta} + \tau_{\theta z}\gamma_{\theta z}\right),$$
$$\delta U = 2\pi R \iint \left(\sigma_x\delta\varepsilon_x + \sigma_\theta\delta\varepsilon_\theta + \tau_{xz}\delta\gamma_{xz}\right)\left(1 + \frac{z}{R}\right) dx dz,$$
$$W = \iint (Pu)\, r d\theta dz = \int P\left(u_0 + zu_1\right)(R + z)\, d\theta dz = \int \left(Pu_0Rh + \frac{Pu_1h^3}{12}\right) d\theta,$$
$$\delta W = 2\pi\left(PRh\delta u_0 + \frac{Ph^3}{12}\delta u_1\right), \tag{3}$$

where $U^* =$ strain energy density. The Hook's stress-strain relations are:

$$\sigma_x = \alpha\left[(1-\nu)\varepsilon_x + \nu\varepsilon_\theta\right], \quad \sigma_\theta = \alpha\left[(1-\nu)\varepsilon_\theta + \nu\varepsilon_x\right],$$
$$\tau_{xz} = \kappa G\gamma_{xz}, \quad \alpha = \frac{E}{(1+\nu)(1-2\nu)}, \tag{4}$$

where $\kappa =$ shear correction factor which it is assumed 5/6.

The stress resultants are defined as:

$$N_x = \int_{-\frac{h}{2}}^{\frac{h}{2}} \sigma_x\left(1 + \frac{z}{R}\right) dz = \alpha h(1-\nu)\frac{du_0}{dx} + \frac{\alpha h(1-\nu)}{2}\left(\frac{dw_0}{dx}\right)^2 + \frac{\alpha(1-\nu)}{R}\frac{h^3}{12}\frac{du_1}{dx} + \frac{\alpha\nu h}{R}w_0,$$
$$M_x = \int_{-\frac{h}{2}}^{\frac{h}{2}} z\sigma_x\left(1 + \frac{z}{R}\right) dz = \frac{\alpha(1-\nu)h^3}{12}\frac{du_1}{dx} + \frac{\alpha(1-\nu)}{R}\frac{h^3}{12}\frac{du_0}{dx} + \frac{\alpha(1-\nu)}{R}\frac{h^3}{24}\left(\frac{dw_0}{dx}\right)^2,$$
$$N_\theta = \int_{-\frac{h}{2}}^{\frac{h}{2}} \sigma_\theta dz = \alpha(1-\nu)mw_0 + \alpha\nu h\frac{du_0}{dx} + \frac{\alpha\nu h}{2}\left(\frac{dw_0}{dx}\right)^2, \quad m = \ln\left(\frac{R + \frac{h}{2}}{R - \frac{h}{2}}\right),$$
$$Q_x = \int_{-\frac{h}{2}}^{\frac{h}{2}} \tau_{xz}\left(1 + \frac{z}{R}\right) dz = Gh\frac{dw_0}{dx} + Ghu_1. \tag{5}$$

The equilibrium equation is obtained as the following:

$$\frac{dN_x}{dx}=0,\quad -\frac{dM_x}{dx}+Q_x=0,\quad \frac{d}{dx}\left(N_x\frac{dw_0}{dx}\right)+\frac{N_\theta}{R}-\frac{dQ_x}{dx}=0. \tag{6}$$

The boundary conditions are:

$$\begin{aligned}&2\pi RN_x\delta u_0|_{x=0..l}=2\pi RPh\delta u_0|_{x=0..l},\\&2\pi RM_x\delta u_1|_{x=0..l}=\frac{2\pi h^3}{12}P\delta u_1|_{x=0..l},\\&2\pi RN_x\frac{dw_0}{dx}\delta w_0|_{x=0..l}+2\pi RQ_x\delta w_0|_{x=0..l}=0.\end{aligned} \tag{7a}$$

From Eqs. (7a), it can conclude the following relations at the edges:

$$\begin{aligned}N_x=Ph\quad&\text{or}\quad u_0=0,\\RM_x=\frac{h^3}{12}P\quad&\text{or}\quad u_1=0,\\N_x\frac{dw_0}{dx}+Q_x=0\quad&\text{or}\quad w_0=0.\end{aligned} \tag{7b}$$

By substituting Eqs. (5) into Eqs. (6) the equilibrium equations are derived as the following. In extracting the first equation, we integrated the first equation (6) and we used the boundary conditions too.

$$\begin{aligned}&Rh\frac{du_0}{dx}+\frac{Rh}{2}\left(\frac{dw_0}{dx}\right)^2+\frac{h^3}{12}\frac{du_1}{dx}+\frac{\nu h}{(1-\nu)}w_0=\frac{RPh}{\alpha(1-\nu)},\\&-\frac{Rh^3}{12}\frac{d^2u_1}{dx^2}-\frac{h^3}{12}\frac{d^2u_0}{dx^2}-\frac{h^3}{12}\frac{dw_0}{dx}\frac{d^2w_0}{dx^2}+\frac{G}{\alpha(1-\nu)}Rh\left(\frac{dw_0}{dx}+u_1\right)=0,\\&-\frac{PRh}{(1-\nu)\alpha}\frac{d^2w_0}{dx^2}+mw_0+\frac{\nu}{1-\nu}h\frac{du_0}{dx}+\frac{\nu}{1-\nu}\frac{h}{2}\left(\frac{dw_0}{dx}\right)^2-\frac{(1-2\nu)Rh}{2(1-\nu)}\left(\frac{d^2w_0}{dx^2}+\frac{du_1}{dx}\right)=0.\end{aligned} \tag{8}$$

These equations contain three coupled nonlinear differential equations.

3 Analytical solution

Equations (8) are solved analytically using the perturbation technique. At first, the following dimensionless parameters are introduced:

$$\begin{aligned}&u_0^*=\frac{u_0}{h_0},\quad h^*=\frac{h}{h_0},R^*=\frac{R}{R_0},\quad w_0^*=\frac{w_0}{h_0},Z=\frac{l^2}{R_0h_0},\quad z_1=\varepsilon Z=\frac{l}{R_0},\\&\beta=\frac{1-2\nu}{2(1-\nu)},\quad x^*=\frac{x}{l},\quad \varepsilon=\frac{h_0}{l},\quad P^*=\frac{P}{(1-\nu)\alpha},\end{aligned} \tag{9}$$

where $h_0=$ thickness characteristic, $R_0=$ radius characteristic, $Z=$ Batdorf parameter, and (*) stands for a dimensionless quantity. ε is a small parameter. By defining $V=\varepsilon\frac{du_0^*}{dx^*}$ and $\eta=\frac{x^*}{\varepsilon}$, the dimensionless form of Eqs. (8) are obtained as the following:

$$\begin{aligned}&R^*h^*V+\frac{R^*h^*}{2}\left(\frac{dw_0^*}{d\eta}\right)^2+\frac{h^{*3}z_1}{12}\varepsilon\frac{du_1^*}{d\eta}+\frac{\nu h^*z_1}{(1-\nu)}\varepsilon w_0^*=h^*R^*P^*,\quad m^*=\ln\left(\frac{R^*+\varepsilon^2z\frac{h^*}{2}}{R^*-\varepsilon^2z\frac{h^*}{2}}\right),\\&-\frac{h^{*3}z_1}{12}\varepsilon\frac{dV}{d\eta}-\frac{R^*h^{*3}}{12}\frac{d^2u_1^*}{d\eta^2}-\frac{h^{*3}z_1}{12}\varepsilon\frac{dw_0^*}{d\eta}\frac{d^2w_0^*}{d\eta^2}+\beta R^*h^*\left(\frac{dw_0^*}{d\eta}+u_1^*\right)=0,\\&\varepsilon\frac{\nu h^*z_1}{1-\nu}V-\beta h^*R^*\frac{du_1^*}{d\eta}-(h^*R^*P^*+\beta h^*R^*)\frac{d^2w_0^*}{d\eta^2}+\varepsilon m^*z_1w_0^*+\frac{\nu h^*z_1}{2(1-\nu)}\varepsilon\left(\frac{dw_0^*}{d\eta}\right)^2=0.\end{aligned} \tag{10}$$

The solution is considered as the following uniform series:

$$V(\eta) = \phi_0(\eta) + \varepsilon\phi_1(\eta) + \ldots, w_0^*(\eta) = \psi_0(\eta) + \varepsilon\psi_1(\eta) + \ldots,$$
$$u_1^*(\eta) = \lambda_0(\eta) + \varepsilon\lambda_1(\eta) + \ldots. \tag{11}$$

By considering the same order terms of ε, the following equations obtain. For order-zero:

$$\phi_0(\eta) + \frac{1}{2}\left(\frac{d\psi_0(\eta)}{d\eta}\right)^2 - P^* = 0,$$
$$h^*R^*\beta\frac{d\psi_0(\eta)}{d\eta} - \frac{R^*h^{*3}}{12}\frac{d^2\lambda_0(\eta)}{d\eta^2} + h^*R^*\beta\lambda_0(\eta) = 0,$$
$$-h^*R^*\beta\frac{d\lambda_0(\eta)}{d\eta} - h^*R^*(\beta + P^*)\frac{d^2\psi_0(\eta)}{d\eta^2} = 0. \tag{12}$$

For order-one:

$$R^*h^*\left(\frac{d\psi_1(\eta)}{d\eta}\right)\left(\frac{d\psi_0(\eta)}{d\eta}\right) + \frac{h^{*3}z_1}{12}\frac{d\lambda_0(\eta)}{d\eta} + R^*h^*\phi_1(\eta) - \frac{z_1\nu h^*}{(\nu-1)}\psi_0(\eta) = 0,$$
$$-\frac{h^{*3}z_1}{12}\frac{d\phi_0(\eta)}{d\eta} - \frac{h^{*3}z_1}{12}\left(\frac{d^2\psi_0(\eta)}{d\eta^2}\right)\left(\frac{d\psi_0(\eta)}{d\eta}\right)$$
$$+\beta R^*h^*\frac{d\psi_1(\eta)}{d\eta} - \frac{h^{*3}z_1}{12}\frac{d^2\lambda_1(\eta)}{d\eta^2} + \beta R^*h^*\lambda_1(\eta) = 0,$$
$$\frac{z_1\nu h^*}{2(\nu-1)}\left(\frac{d\psi_0(\eta)}{d\eta}\right)^2 - \beta R^*h^*\frac{d\lambda_1(\eta)}{d\eta} - h^*R^*(\beta + P^*)\frac{d^2\psi_1(\eta)}{d\eta^2} - \frac{z_1\nu h^*}{(\nu-1)}\phi_0(\eta) = 0. \tag{13}$$

From Eqs. (12), one can result: $\phi_0 = P^*$, $\psi_0 = 0$, $\lambda_0 = 0$. By inserting these values into Eqs. (13), one can result:

$$[A]_2\frac{d^2\{Y\}}{d\eta^2} + [A]_1\frac{d\{Y\}}{d\eta} + [A]_0\{Y\} + \{F\} = \{0\},$$
$$\{Y\} = [\lambda_1, \psi_1]^T, \quad \{F\} = \begin{bmatrix}0 & -\frac{h^*Z_1\nu P^*}{(\nu-1)}\eta + c1\end{bmatrix}^T, \quad [A]_0 = \begin{bmatrix}\beta R^*h^* & 0\\ -\beta R^*h^* & 0\end{bmatrix},$$
$$[A]_1 = \begin{bmatrix}0 & \beta R^*h^*\\ 0 & -R^*h^*(\beta + P^*)\end{bmatrix}, \quad [A]_2 = \begin{bmatrix}-\frac{R^*h^{*3}}{12} & 0\\ 0 & 0\end{bmatrix}. \tag{14}$$

Equations (14) are a system of the ordinary differential equations with constant coefficients. By considering the general solution as $\{Y\} = \{C\}e^{n\eta}$ and substituting into Eqs. (14), it is resulted:

$$\left([A]_2n^2 + [A]_1n + [A]_0\right)\{C\} = \{0\}. \tag{15}$$

The eigenvalues n can calculate from the determinant of the system matrix. So, the general solution is in the form of $\{Y\}_g = \sum_{i=1}^{6} d_i\{C\}_i e^{n_i\eta}$. The particular solution can determine easily from the differential equation theory. The constants d_i obtain from the boundary conditions.

4 Stability equations

For extracting the stability equations, the following increments are considered for the displacement components of Eq. (1):

$$u_0(x) = u_{00} + u_{01}, u_1(x) = u_{10} + u_{11}, w_0(x) = w_{00} + w_{01}. \tag{16}$$

In Eqs. (16) u_{00}, u_{10}, and w_{00} are the components of displacements in equilibrium position which satisfy Eqs. (8) and u_{01}, u_{11}, w_{01} are their *small* increments. By substituting Eqs. (16) into Eqs. (8) the stability equations are derived as the following:

$$\alpha h\left(1-\nu\right)\frac{du_{01}}{dx}+\frac{\alpha h\left(1-\nu\right)}{2}\left(2\frac{dw_{00}}{dx}\frac{dw_{01}}{dx}\right)+\frac{\alpha h^{3}\left(1-\nu\right)}{12R}\frac{du_{11}}{dx}+\frac{\alpha\nu h}{R}w_{01}=0,$$

$$\frac{\alpha\left(1-\nu\right)h^{3}}{12}\frac{d^{2}u_{11}}{dx^{2}}+\frac{\alpha\left(1-\nu\right)h^{3}}{12R}\frac{d^{2}u_{01}}{dx^{2}}+\frac{\alpha\left(1-\nu\right)h^{3}}{12R}\frac{d}{dx}\left(\frac{dw_{00}}{dx}\frac{dw_{01}}{dx}\right)+Gh\left(\frac{dw_{01}}{dx}+u_{11}\right)=0,$$

$$\begin{aligned}&\left(\alpha h\left(1-\nu\right)\frac{du_{00}}{dx}\frac{d^{2}w_{01}}{dx^{2}}+\frac{\alpha\left(1-\nu\right)h^{3}}{12R}\frac{du_{10}}{dx}\frac{d^{2}w_{01}}{dx^{2}}+\frac{\alpha\nu h}{R}w_{00}\frac{d^{2}w_{01}}{dx^{2}}\right.\\&\quad\left.+\alpha h\left(1-\nu\right)\frac{du_{01}}{dx}\frac{d^{2}w_{00}}{dx^{2}}+\frac{\alpha\left(1-\nu\right)h^{3}}{12R}\frac{du_{11}}{dx}\frac{d^{2}w_{00}}{dx^{2}}+\alpha h\left(1-\nu\right)\left(\frac{dw_{00}}{dx}\frac{dw_{01}}{dx}\frac{d^{2}w_{00}}{dx^{2}}\right)\right)\\&\quad+\frac{\alpha m\left(1-\nu\right)}{R}w_{01}+\frac{\alpha\nu h}{R}\frac{du_{01}}{dx}+\frac{\alpha\nu h}{R}\left(\frac{dw_{00}}{dx}\frac{dw_{01}}{dx}\right)-Gh\left(\frac{d^{2}w_{01}}{dx^{2}}+\frac{du_{11}}{dx}\right)=0.\end{aligned}\tag{17}$$

Due to smallness of u_{01}, u_{11}, w_{01} one can ignore the higher orders of this terms. Equations (17) contain three *coupled ordinary differential equations with variable coefficients*. Brush [1] presented this method for extracting the stability equations.

5 Analytical solution

The stability equations are solved for the bifurcating point. At this point, $w_{00}=0$, and from the solution of the equilibrium equation $u_{10}=0$, $\varepsilon\frac{du_{00}}{dx}=P^{*}$. By substituting these values into Eqs. (17), one can rewrite the stability equations in the following dimensionless form.

$$\begin{aligned}&[B]_{2}\frac{d^{2}\{Y\}}{d\eta^{2}}+[B]_{1}\frac{d\{Y\}}{d\eta}+[B]_{0}Y=\{0\},\quad\{Y\}=[u_{11},w_{01},u_{01}]^{T},\\&[B]_{0}=\begin{bmatrix}0&\frac{\nu h^{*}z_{1}}{R^{*}}\varepsilon&0\\\frac{Gh^{*}}{\alpha}&0&0\\0&\frac{\alpha(1-\nu)mz_{1}}{R^{*}}\varepsilon&0\end{bmatrix},\quad[B]_{1}=\begin{bmatrix}\frac{h^{*3}(1-\nu)z_{1}}{12R^{*}}\varepsilon&0&h^{*}\left(1-\nu\right)\\0&\frac{G}{\alpha}h^{*}&0\\-Gh^{*}&0&\frac{\alpha\nu h^{*}z_{1}}{R^{*}}\varepsilon\end{bmatrix},\\&[B]_{2}=\begin{bmatrix}0&0&0\\-\frac{h^{*3}(1-\nu)}{12}&0&-\frac{h^{*3}(1-\nu)z_{1}}{12R^{*}}\\0&-(\alpha h^{*}\left(1-\nu\right)P^{*}+Gh^{*})&0\end{bmatrix}.\end{aligned}\tag{18}$$

Equations (18) are a system of homogeneous differential equations. With applying the boundary conditions, it is possible to find the buckling load which are the eigenvalues of Eqs. (18).

6 Numerical analysis

Ansys 11 FE package is used for the numerical analysis. SHELL93 element which includes 8 nodes with 6 degree-of-freedom in each node and it can model the large deflection behavior is used for discritization. Figure 2 shows the mesh pattern and loading of the shell. The mesh size is selected by trial and error to vanish the sensitivity of the results to mesh size variations. The boundary conditions at $x=0$ is clamped but at $x=l$, just the radial displacement is constraint. Also, for monitoring the results through the thickness, one can use PLANE82 element in axisymmetric mode, which is a quadrilateral element with 8 nodes and two degree-of-freedom in each node and its equations are derived using three-dimensional theory of elasticity. SHELL93 does not report the displacements variations through thickness and its output contains the middle surface displacements.

7 Results

For discussing the results, some parametric studies were performed. In all cases, the Young's modulus and the Poisson's ratio are $E=200$ GPa, $\nu=0.3$, respectively. The analytical solution was done on Maple 13 environment. Figures 3 and 4 show the dimensionless displacements of the shell which are defined as $U*x=Ux/h_{0}$, $U*z=Uz/h_{0}$ before buckling with respect to non-dimensional distance x^{*} with the numerical and analytical methods. The maximum difference between the axial displacement results is about 9%. In addition, the radial displacement is very small with respect to the axial displacement.

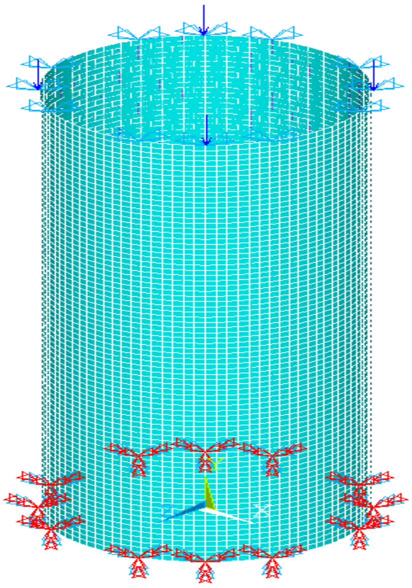

Fig. 2 (online colour at: www.zamm-journal.org) Mesh pattern.

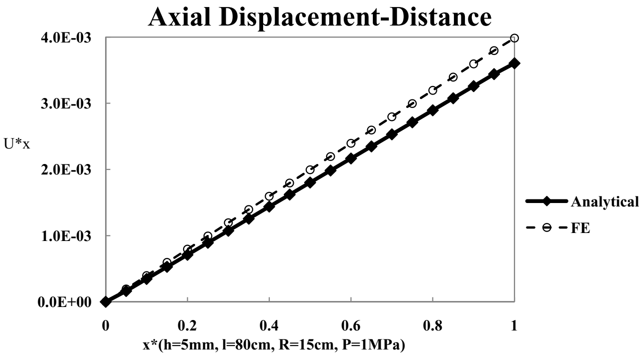

Fig. 3 Dimensionless axial displacement – comparison with FE method.

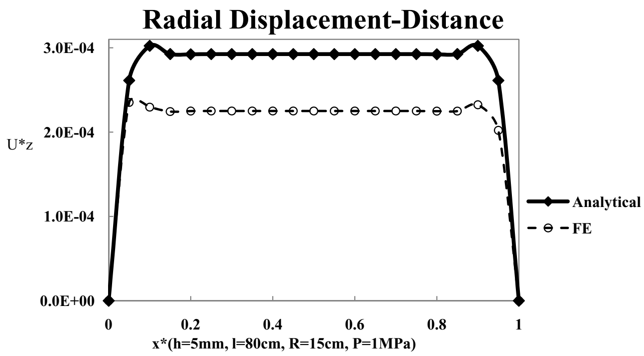

Fig. 4 Dimensionless radial displacement – comparison with FE method.

Figure 5 shows the effect of R/h on dimensionless buckling stress. The results have compared with the FE method and the classical (Lorenz) formula for buckling stress i.e. $\sigma = 0.605\,\frac{E\,h}{R}$ for $\nu = 0.3$ [10]. The difference between the analytical and FE results decreases for large values R/h. The analytical buckling stress is larger than the FE one and the analytical solution is more accurate than the classical formula with respect to the FE results. In addition, the shear deformation theory cannot improve the classical theory results for large values of R/h.

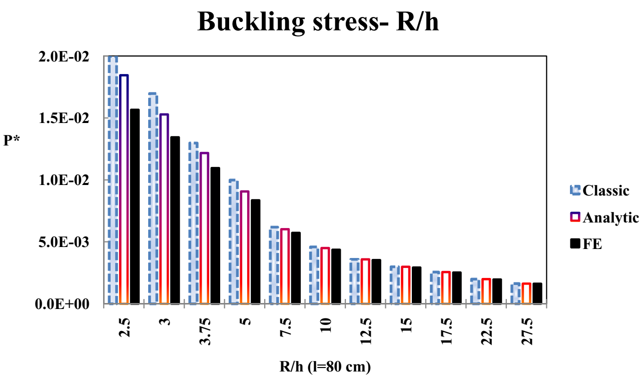

Fig. 5 (online colour at: www.zamm-journal.org) Effect of R/h on dimensionless buckling stress.

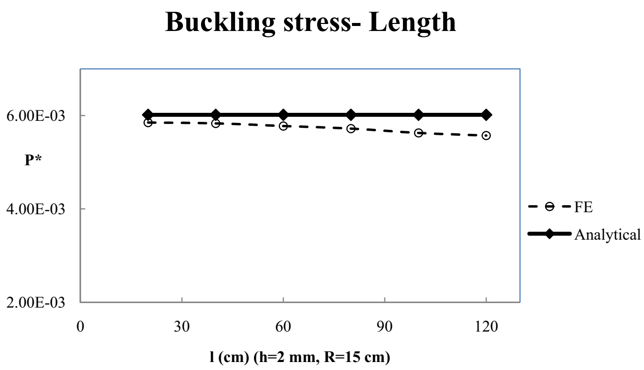

Fig. 6 Effect of the length on the buckling stress – comparison with FE method.

Figure 6 presents the effect of the length variations on the buckling stress. There is no change in the buckling stress in analytical solution. It is correct in classical theory too i.e. the classical formula does not depend to the length (except that the short cylinders) . In FE graph, a slow decrease is seen by increasing the length. Figure 7 shows the effect of the mean radius on the buckling stress. It decreases by enlarging the radius. The differences between FE and analytical results are more for thick shells. According to trend line of the graph, the buckling stress is proportion to $R^{-0.93}$ for analytical solution, $R^{-0.88}$ for FE results (which is not shown) and R^{-1} for the classical theory. The variations of the non-dimensional axial displacements through the thickness are plotted in Fig. 8. for different values of thicknesses with the FE method by using PLANE82 element. From Fig. 8. it is seen that by increasing the thickness, Eq. (1) which is a linear equation with respect to z is not correct. It is possible to find a validation range of thickness for Eq. (1) by trial and error. Figure 8 is drawn near the boundary $x^* = 0.002$ and one can expect more linearity behavior far the boundaries.

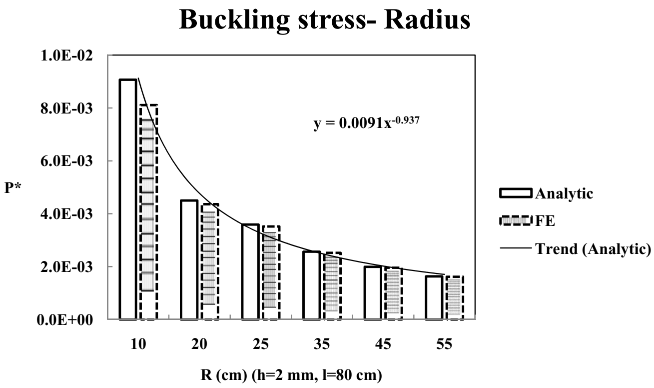

Fig. 7 (online colour at: www.zamm-journal.org) Effect of the radius on buckling stress – comparison with FE method.

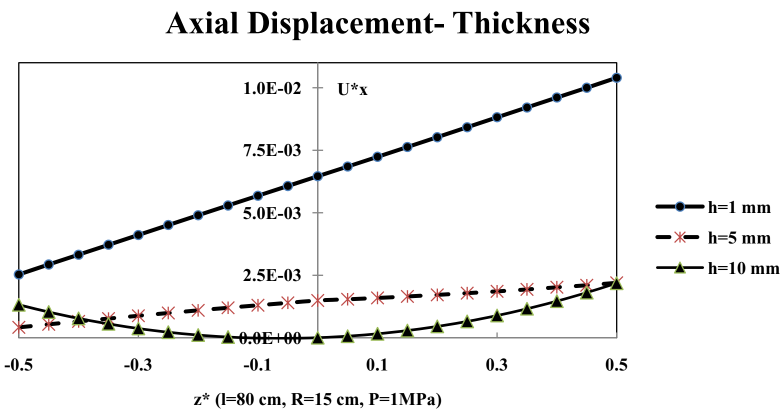

Fig. 8 (online colour at: www.zamm-journal.org) Dimensionless axial displacement through thickness with FE method ($x^* = 0.002$).

In Table 1 the buckling stress has been obtained with various methods and the difference percentage with respect to the FE method has been calculated. It is obvious that by increasing the thickness, the difference increases but the shear deformation theory has smaller difference with respect to the classical theory.

Table 1 Buckling load ($l = 80$ cm, $R = 10$ cm).

Method	h (mm)	P_{cr} (Pa)	Difference percentage with respect to FE
Analytical	1	1.21e9	6.1%
FE	212	1.14e9	0
Classical theory [10]	1	1.21e9	6.1%
Analytical	5	5.26e9	17.9%
FE	5	4.46e9	0
Classical theory	5	6.05e9	35.7%
Analytical	10	1.006e10	25.8%
FE	10	8e9	0
Classical theory	10	1.21e10	51.3%

8 Conclusion

An analytical method based on the perturbation technique was proposed to find the buckling load and displacements of a cylindrical shell by using the first order shear deformation theory. The results show that the first order theory is more effective than the classical theory to find the buckling load and displacements of thin or moderately thick shells. It is possible to prepared a simple program on Maple environment for these calculations and performing a parametric study to investigate the effects of geometrical parameters of shell on the buckling load. It is easier and faster than the FE method to obtain the buckling load, because it does not need to create a FE model.

References

[1] D. O. Brush and B. O. Almroth, Buckling of Bars, Plates and Shells (McGraw-Hill, New York, 1975).
[2] M. Cai, J. Holst, and J. Rotter, Buckling Strength of Thin Cylindrical Shells Under Localized Axial Compression, 15th ASCE Engineering Mechanics Conference, (Columbia University, New York, 2002).
[3] A. Khamlichi, M. Bezzazi, and A. Limam, Buckling of elastic cylindrical shells considering the effect of localized axisymmetric imperfections, Thin-Walled Struct. **42**, 1035–1047 (2004).
[4] S. Aghajari, K. Abedi, and H. Showkati, Buckling and post-buckling behavior of thin-walled cylindrical steel shells with varying thickness subjected to uniform external pressure, Thin-Walled Struct. **44**, 904–909 (2006).
[5] R. Abdelmoula and A. Leger, Singular perturbation analysis of the buckling of circular cylindrical shells, Eur. J. Mech. A, Solids **27**, 706–729 (2008).
[6] H. Shen and Y. Xiang, Buckling and post-buckling of anisotropic laminated cylindrical under combined axial compression and torsion, Compos. Struct. **84**, 375–386 (2008).
[7] H. Shen, Torsional buckling and post-buckling of FGM cylindrical shells in thermal environments, Int. J. Non-linear Mech. **44**, 644–657 (2009).
[8] Z. Li and Z. Lin, Non-linear buckling and post-buckling of shear deformable anisotropic laminated cylindrical shell subjected to varying external pressure loads, Compos. Struct. **92**, 553–567 (2010).
[9] M. Ambali, Nonlinear Vibrations and Stability of Shells and Plates (Cambridge University Press, Cambridge, 2008).
[10] S. P. Timoshenko and J. M. Gere, Theory of Elastic Stability, 2nd Edition (McGraw-Hill, New York, 1963).